Journal of Solid State Chemistry 184 (2011) 965–970

Contents lists available at ScienceDirect

Journal of Solid State Chemistry

journal homepage: www.elsevier.com/locate/jssc

Preparation, crystal structure and photoluminescence of garnet-type calcium tin titanium aluminates

Hisanori Yamane *, Tetsuya Kawano

Institute of Multidisciplinary Research for Advanced Materials, Tohoku University, 2-1-1 Katahira, Aoba-ku, Sendai 980-8577, Japan

ARTICLE INFO

Article history:
Received 21 December 2010
Received in revised form
6 February 2011
Accepted 16 February 2011
Available online 26 February 2011

Keywords:
Garnet structure
X-ray diffraction
Single crystal
Rietveld refinement
Photoluminescence spectra

ABSTRACT

Colorless and transparent single crystals of $Ca_3Sn_{2.2}Ti_{0.8}Al_2O_{12}$, which emit blue–white light under ultraviolet light, were prepared by heating a mixture of oxides and calcium carbonate with a calcium and aluminum-rich composition at 1500 °C. Single crystal X-ray diffraction revealed that the crystal structure is the garnet-type with a cubic cell parameter (a=12.5309(3) Å) and the space group, $Ia\bar{3}d$ ($R1$=0.0277, $wR2$=0.0663, and S=1.367 for all data). The structural formula is presented as $Ca_3[Sn_{0.96}Ti_{0.04}]_{octa}[Al_{0.67}Ti_{0.24}Sn_{0.09}]_{tetra}O_{12}$. Polycrystalline solid solutions of $Ca_3Sn_{3-x}Ti_xAl_2O_{12}$ were prepared by solid state reaction in air at 1370 °C with nominal titanium contents from x=0.6 to 1.4. The refined unit cell parameter decreased with increasing x. A broad blue–white emission with a peak wavelength of 465 nm was observed for the solid solutions at room temperature.

1. Introduction

The emission originating from charge transfer (CT) transitions between Ti^{4+} and O^{2-} was observed at room temperature for Sn^{4+} containing oxides such as $A_2Sn_{1-x}Ti_xO_4$ (A=Ca, Sr, and Ba) [1], $BaSn_{0.9}Ti_{0.1}Si_3O_9$ [2], $CaSn_{1-x}Ti_xSiO_5$ [3], $Ca_3Sn_{1-x}Ti_xSi_2O_9$ [3], $CaSn_{1-x}Ti_x(BO_3)_2$ [4], and $Mg_5Sn_{1-x}Ti_xB_2O_{10}$ [5], where Sn^{4+} in oxygen octahedra are partially replaced by Ti^{4+}. Four-fold oxygen-tetrahedral coordination around Sn^{4+} is not so common, but it is realized in K_4SnO_4 [6]. Partial occupation of Sn^{4+} at the oxygen tetrahedral sites with Fe^{3+}, Ge^{4+}, or Si^{4+} has been reported for the garnet-type oxides prepared in the systems of $CaO–Fe_2O_3–TiO_2–SnO_2$ [7], $CaO–Fe_2O_3–Y_2O_3–SnO_2$ [8], and $CaO–Ga_2O_3–GeO_2–SiO_2–SnO_2$ [9]. In the garnet-type oxides of $Ca_3Sn_{3-x}Ti_xFe_2O_{12}$ [7], $Ca_3Fe_2(Si_{1-x}Ti_x)_3O_{12}$ [10], and $Ca_3In_2(Si,Ti)_3O_{12}$ [10], Ti^{4+} atoms are located at both tetrahedral and octahedral sites. These garnet phases were studied with polycrystalline powder samples. Geller et al. [8] described that $Ca_3Fe_2Sn_3O_{12}$ decomposes into $CaSnO_3$ and α-Fe_2O_3 when it melts. The occupation of Sn^{4+} and Ti^{4+} at the tetrahedral sites of the garnet-type structure has been clarified by powder X-ray diffraction (XRD), Raman spectroscopy, and infrared spectroscopy [7–10]. The luminescence properties of the garnet-type compounds containing Ti^{4+} have not been reported.

Recently, Yamane et al. [11] have prepared single crystals of a new compound $Ca_2Sn_2Al_2O_9$ in the $CaO–Al_2O_3–SnO_2$ system by the self-flux method using a melt with a composition of Ca and Al in excess of that of $Ca_2Sn_2Al_2O_9$, considering the eutectic point of $Ca_3Al_2O_6–CaAl_2O_4$ at 1373 °C [12]. Single crystal XRD analysis revealed that $Ca_2Sn_2Al_2O_9$ is isostructural with $Na_2Ti_2Si_2O_9$ (ramsayite). In the present paper, single crystals of a garnet-type oxide were prepared in the $CaO–Al_2O_3–TiO_2–SnO_2$ system using a Ca and Al-rich starting material. Polycrystalline garnet-type solid solutions of $Ca_3Sn_{3-x}Ti_xAl_2O_{12}$ were prepared by solid state reaction. The crystal structure and photoluminescence (PL) of the single crystals and polycrystalline samples were investigated.

2. Experimental procedure

Starting materials were powders of $CaCO_3$ (99.99%, Rare Metallic), SnO_2 (99.99%, Rare Metallic), TiO_2 (99.99%, Rare Metallic), and α-Al_2O_3 (99.99%, Rare Metallic). The powders were weighed, mixed in an agate mortar with a pestle, and pressed into a pellet. The pellet was placed on a platinum plate and heated in air using an electric furnace. Single crystals of the garnet-type compound were prepared from a starting mixture with an atomic ratio of Ca:Sn:Ti:Al=5:1:1:5. The pellet of the mixture was heated at 1550 °C for 1 h and then cooled at a rate of −5 °C/h. Polycrystalline pellet samples were prepared by heating the starting mixtures with atomic ratios Ca:Sn:Ti:Al=3:3−x:x:2 (x=0–2.0) at 1370 °C for 12 h first, followed by powdering, pellet formation, and heating at the same temperature for 72 h.

* Corresponding author. Fax: +81 22 217 5813.
E-mail address: yamane@tagen.tohoku.ac.jp (H. Yamane).

0022-4596/$ - see front matter © 2011 Elsevier Inc. All rights reserved.
doi:10.1016/j.jssc.2011.02.016

XRD data of a single crystal were collected using Mo $K\alpha$ radiation with a graphite monochromator and an imaging plate on a single crystal X-ray diffractometer (Rigaku, Model R-AXIS RAPID-II). Diffraction-data collection and unit-cell refinement were performed by the PROCESS-AUTO program [13]. Absorption correction was performed by the NUMABS program [14]. The crystal structure was refined by the full-matrix least-squares on F^2, using the SHELXL-97 program [15]. All calculations were carried out on a personal computer using the WinGX software package [16]. The crystal structures were illustrated by the VESTA program [17].

The obtained polycrystalline pellets were powdered and the XRD patterns of the powders were measured at a step width of 0.02° in 2θ using Cu $K\alpha$ radiation with a graphite monochromator mounted on a powder diffractometer (Rigaku, Model RINT2000). The crystal structure parameters of the solid solutions were refined using the RIETAN-FP program [18].

Elemental analysis of a single crystal was performed by wavelength dispersive X-ray (WDX) spectroscopy with an electron micro-probe analyzer (JEOL JXA-8200). In the WDX analysis, the atomic composition was calculated by the ZAF (element number, absorption, and fluorescence corrections) quantification method with relative X-ray intensities observed from the sample and the standard samples of $CaSiO_3$, SnO_2, TiO_2, Al_2O_3, and TiO_2.

Table 1
Crystal data and structure refinement for $Ca_3Sn_{2.2}Ti_{0.8}Al_2O_{12}$ with single crystal XRD data.

Chemical formula	$Ca_3Sn_{2.2}Ti_{0.8}Al_2O_{12}$
Formula weight, M_r	665.64 g mol^{-1}
Temperature, T	298(2) K
Crystal system, space group	Cubic, $Ia\bar{3}d$ (No. 230)
Unit cell parameter	a=12.5309(3) Å
Unit-cell volume	1967.65(8) Å^3
Z	8
Calculated density, D_{cal}	4.494 Mg m^{-3}
Radiation wavelength, λ	0.71075 Å (Mo $K\alpha$)
Absorption coefficient, μ	7.988 mm^{-1}
F_{000}	2477
Crystal size	0.23 × 0.22 × 0.21 mm^3
θ range for data collection	3.98–30.49°
Limiting indices	$-17 \le h \le 11$, $-17 \le k \le 14$, $-17 \le l \le 15$
Reflections collected/unique	10602/255 [R(int)=0.0484]
Absorption correction	numerical
Data/restraints/parameters	255/2/21
Goodness-of-fit on F^2, S	1.367
R indices [$I > 2\sigma(I)$] $R1$, $wR2$	0.0262, 0.0657
R indices (all data) $R1$, $wR2$	0.0277, 0.0663
Largest diffr. peak and hole, $\Delta\rho$	0.51 and −0.96 e/Å^3

$R1=\Sigma||F_o|-|F_c||/\Sigma|F_o|$. $wR2=[\Sigma w\cdot(F_o^2-F_c^2)^2/\Sigma(w\cdot F_o^2)^2]^{1/2}$, $w=1/[\sigma^2\cdot(F_o^2)+(0.0175P)^2+23.1963P]$ where F_o is the observed structure factor, F_c is the calculated structure factor, σ is the standard deviation of F_c^2, and $P=(F_o^2+2F_c^2)/3$. $S=[\Sigma w\cdot(F_o^2-F_c^2)^2/(n-p)]^{1/2}$, where n is the number of reflections and p is the total number of parameters refined.

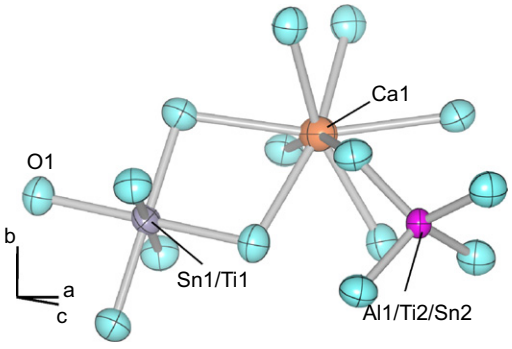

Fig. 1. O1-atom coordination around the Ca1, Sn1/Ti1 and Al1/Ti1/Sn1 sites in the structure of $Ca_3Sn_{2.2}Ti_{0.8}Al_2O_{12}$. Displacement ellipsoids are drawn at 99% probability level.

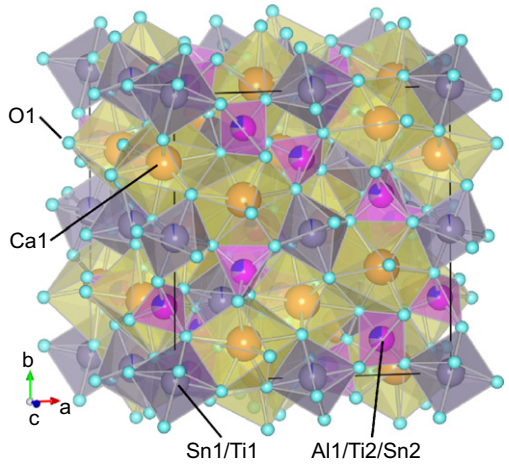

Fig. 2. Crystal structure of $Ca_3Sn_{2.2}Ti_{0.8}Al_2O_{12}$ illustrated with Ca1, Sn1/Ti1 and Al1/Ti2/Sn2 cation site-centered oxygen polyhedra.

Table 2
Atomic coordinates and equivalent isotropic displacement parameter U_{eq}(Å^2) for $Ca_3Sn_{2.2}Ti_{0.8}Al_2O_{12}$.

Atom	Site	Occupancy	x	y	z	U_{eq}[a]
Ca1	24c	1.0	1/8	0	0	0.0102(4)
Sn1/Ti1	16a	0.964(11)/ 0.036(11)	0	0	0	0.0068(2)
Al1/Ti2/Sn2	24d	0.667/0.242(6)/0.091(6)	3/8	0	1/4	0.0059(5)
O1	96h	1.0	0.09774(19)	0.19914(19)	0.28296(19)	0.0094(5)

[a] $U_{eq}=(\sum_i\sum_j U_{ij}a_i^*a_j^*\boldsymbol{a}_i\cdot\boldsymbol{a}_j)/3$.

Table 3
Anisotropic displacement parameters U_{ij} (Å^2) for $Ca_3Sn_{2.2}Ti_{0.8}Al_2O_{12}$.

Atom	U_{11}	U_{22}	U_{33}	U_{12}	U_{13}	U_{23}
Ca1	0.0089(6)	0.0109(4)	0.0109(4)	0.0021(4)	0	0
Sn1/Ti1	0.0068(2)	0.0068(2)	0.0068(2)	−0.00099(10)	−0.00099(10)	−0.00099(10)
Al1/Ti2/Sn2	0.0047(7)	0.0065(5)	0.0065(5)	0	0	0
O1	0.0080(11)	0.0094(11)	0.0107(11)	0.0003(8)	0.0006(8)	−0.0009(8)

The PL excitation and emission spectra of the single crystals and solid solutions were measured at room temperature with a fluorescence spectrometer (Hitachi, F-4500) equipped with a 150-W xenon lamp as an excitation source. The quantum efficiencies of the solid solutions were measured using a quantum efficiency measurement system (Otsuka Electronics, Model QE-1000).

Table 4
Ti content x in the starting mixture of $Ca_3Sn_{3-x}Ti_xAl_2O_{12}$ and products prepared at 1370 °C.

Sample no.	x	Phases in the product
1	0.0	R, P
2	0.2	R, G, P
3	0.4	G, L, P
4	0.6	G, (tr P)
5	0.8	G, (tr P)
6	1.0	G, (tr P)
7	1.2	G, (tr P)
8	1.4	G, (tr P)
9	1.6	G, P, $CaAl_{12}O_{19}$
10	1.8	G, P, $CaAl_{12}O_{19}$, $CaAl_4O_7$
11	2.0	G, P, $CaAl_{12}O_{19}$, $CaAl_4O_7$

G: garnet-type phase, P: perovskite-type phase, R: ramsayite-type phase, and tr: trace amount

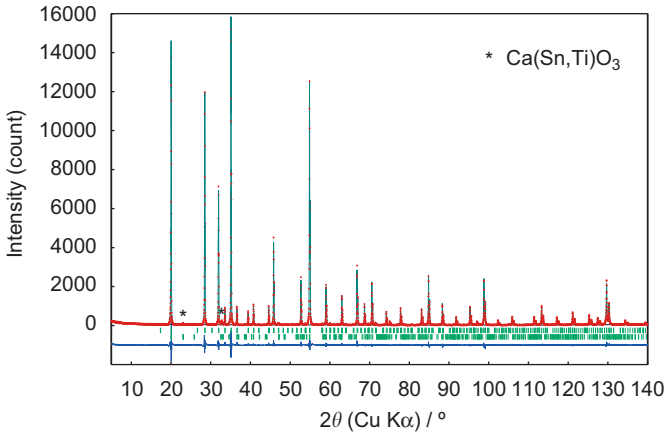

Fig. 3. Observed (dots) and calculated (solid line) powder XRD patterns of $Ca_3SnTiAl_2O_{12}$. Upper and lower vertical lines show the Bragg peak positions of $Ca_3SnTiAl_2O_{12}$ and $Ca(Sn,Ti)O_3$ perovskite phase, respectively. Difference (solid line) is shown at the bottom of the figure. The main reflections of $Ca(Sn,Ti)O_3$ pervskite phase are indicated with the marks (*).

3. Results and discussion

3.1. Single crystal of $Ca_3Sn_{2.2}Ti_{0.8}Al_2O_{12}$

Colorless and transparent single crystals with a size of around 0.2 mm were obtained by crushing the sample which was solidified after melting by cooling. The single crystals emitting blue–white light under ultraviolet (UV) light radiation were selected.

The crystal data and structure refinement of the garnet-type single crystal are shown in Table 1. Observed XRD reflections were indexed with a cubic cell parameter (a=12.5309(3) Å, the space group, $Ia\bar{3}d$). Table 2 lists the refined positional parameters and equivalent isotropic displacement parameters. The anisotropic displacement parameters are shown in Table 3. Postulating the garnet-type structure with a composition of $Ca_3Sn_{3-x}Ti_xAl_2O_{12}$, the 24*c* and 96*h* sites are fully occupied by Ca and O atoms, respectively. The occupancies of Sn and Ti atoms at the 16*a* octahedral site and the 24*d* tetrahedral site were refined by assuming that the Al atom is only at the tetrahedral site of 24*d*. The structure was refined with good final R indices of $R1$=0.0277 and $wR2$=0.0663 for all data. The chemical formula determined by this refinement was $Ca_3Sn_{2.2}Ti_{0.8}Al_2O_{12}$. The chemical

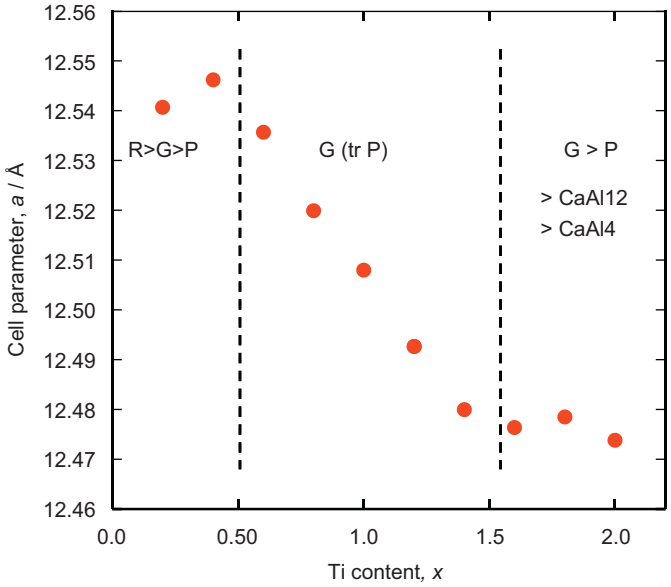

Fig. 4. Unit cell parameters of $Ca_3Sn_{3-x}Ti_xAl_2O_{12}$ plotted as a function of Ti content x in the starting mixture. (G: garnet-type phase, P: perovskite-type phase, R: ramsayite-type phase, CaAl12: $CaAl_{12}O_{19}$, and CaAl4:$CaAl_4O_7$.)

Table 5
Results of the Rietveld analysis and crystal structure data for $Ca_3Sn_{3-x}Ti_xAl_2O_{12}$.

Crystal system	Cubic				
Space group	$Ia\bar{3}d$				
Z	8				
Ti content, x	0.6	0.8	1.0	1.2	1.4
Unit cell parameter (Å)	12.53570(8)	12.51992(6)	12.50801(10)	12.49272(9)	12.47999(10)
Unit cell volume V (Å^3)	1969.91(2)	1962.477(16)	1956.88(3)	1949.71(2)	1943.76(3)
R indices					
R_{wp}	0.1100	0.1154	0.1109	0.1126	0.1090
R_P	0.0730	0.0794	0.0728	0.0746	0.0741
R_B	0.0209	0.0234	0.0160	0.0173	0.0197
R_F	0.0185	0.0246	0.0204	0.0148	0.0150
Goodness-of-fit, S	1.3914	1.4270	1.4499	1.4419	1.4309

R_{wp}, R_P, R_B, R_F, and S are defined in [24].

composition of Ca 18.1, Sn 39.2, Ti 5.9, Al 8.1, and O 28.8 mass% calculated from this formula was close to the composition of Ca 18.2(5), Sn 40.5(8), Ti 4.8(34), Al 9.4(9), and O 27.1(8) mass% measured by WDX analysis.

The coordination environments of the Ca1, Sn1/Ti1, and Al1/Ti2/Sn2 sites are drawn with displacement ellipsoids in Fig. 1. The crystal structure of $Ca_3Sn_{2.2}Ti_{0.8}Al_2O_{12}$ is illustrated with the metal atoms-centered oxygen polyhedra in Fig. 2. Nine percent and 24% of the 24*d* tetrahedral sites are occupied by Sn and Ti atoms, respectively. About 4% of the 16*a* octahedral site is occupied by Ti atoms.

The Ca1 atom is coordinated by eight O1 atoms with Ca1–O1 distances of 2.413(2) Å × 4 and 2.552(2) Å × 4. The bond valence sum (BVS) calculated for the Ca1 atom with the bond valence parameter (BVP) of R(Ca–O)=1.967 Å [19] was 2.02, which was consistent with the divalent of Ca(II). The Sn1/Ti1–O1 distance was 2.054 Å × 6. The BVS calculated with the distances and BVP R(Sn–O)=1.905 Å was 4.02, suggesting almost full occupation of the Sn1/Ti1 site by Sn(IV) atoms. The Al1/Ti2/Sn2–O distance of 1.799(2) Å × 4 is around the Al–O distances 1.76–1.78 Å reported for rare-earth aluminum garnets [20] and Ti–O distances of TiO_4 tetrahedra reported for Li_4TiO_4 (1.80–1.87 Å) [21] and Ba_2TiO_4 (1.63–1.82 Å) [22], and shorter than Sn–O distance of 1.947–1.960 Å for the SnO_4 tetrahedron in K_4SnO_4 [6].

3.2. $Ca_3Sn_{3-x}Ti_xAl_2O_{12}$ solid solutions

Ti contents x in the starting mixtures and the products prepared at 1370 °C are summarized in Table 4. The phase relations in the products are plotted in the CaO–SnO_2–TiO_2–Al_2O_3 diagram of the supplement figure (Fig. S1). The sample prepared without Ti (x=0) consisted of ramsayite-type $Ca_2Sn_2Al_2O_9$ and perovskite-type $CaSnO_3$. A garnet-type phase was contained in the sample prepared at x=0.2. The samples of a garnet-type phase with a trace amount of perovskite-type Ca(Sn,Ti)O_3 were prepared at x=0.4–1.4. At and above x=1.6, the XRD reflections of the perovskite-type phase were clearly observed with those of $CaAl_{12}O_{19}$ and $CaAl_4O_7$.

The powder XRD pattern of the sample prepared with x=1.0 is shown in Fig. 3. The main reflections from the perovskite-type phase are indicated by asterisks (*). Rulmont et al. [9] mentioned that the perovskite phase of $CaSnO_3$, which is easily evidenced by X-ray diffraction, is very stable and reacts very slowly with remaining reactants to intermediate products and that it is very difficult to get rid of the last parts of this impurity. Similar to this report, we were not able to obtain the garnet-type solid solutions without traces of the perovskite-type phase. When the garnet-type $Ca_3Sn_{3-x}Ti_xAl_2O_{12}$ prepared at 1370 °C was heated at 1580 °C, it melted and decomposed into a mixture of a perovs-

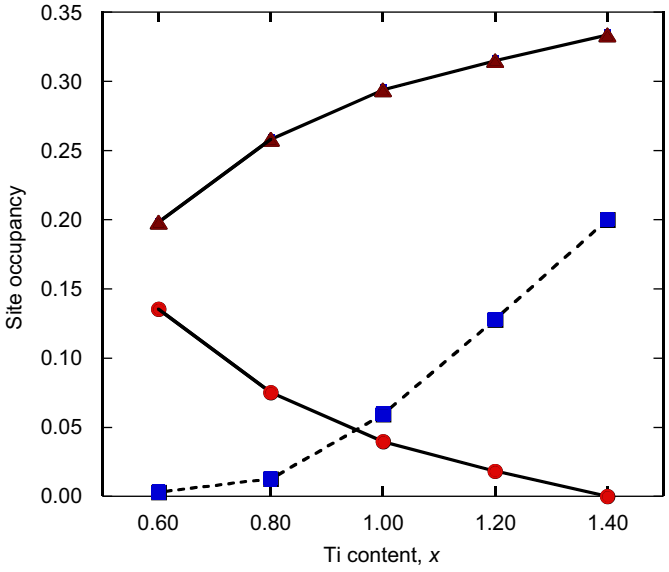

Fig. 5. Occupancy of M=Ti (■) and Sn (●) at the Al1/Ti2/Sn2 (24*d*) site, and Ti (▲) at the Sn1/Ti1 (16*a*) site of $Ca_3Sn_{3-x}Ti_xAl_2O_{12}$ as a function of Ti content x.

Table 6
Site occupancies, atomic coordinates and isotropic atomic displacement parameters for $Ca_3Sn_{3-x}Ti_xAl_2O_{12}$.

Atom	Site	Occ.	x	y	z	B(Å^2)
x=0.6						
Ca1	24*c*	1.0	1/8	0	1/4	0.42(4)
Sn1/Ti1	16*a*	0.9970/0.0030	0	0	0	0.339(11)
Al1/Ti2/Sn2	24*d*	0.6667/0.1980(16)/0.1353	3/8	0	1/4	0.35(5)
O1	96*h*	1.0	0.0983(2)	0.1994(2)	0.2824(2)	0.16(5)
x=0.8						
Ca1	24*c*	1.0	1/8	0	1/4	0.35(4)
Sn1/Ti1	16*a*	0.9872/0.0128	0	0	0	0.309(11)
Al1/Ti2/Sn2	24*d*	0.6667/0.2582(17)/0.0752	3/8	0	1/4	0.34(5)
O1	96*h*	1.0	0.0976(2)	0.1992(2)	0.2822(2)	0.10(5)
x=1.0						
Ca1	24*c*	1.0	1/8	0	1/4	0.54(4)
Sn1/Ti1	16*a*	0.9407/0.0593	0	0	0	0.461(11)
Al1/Ti2/Sn2	24*d*	0.6667/0.2938(16)/0.0396	3/8	0	1/4	0.60(5)
O1	96*h*	1.0	0.0970(2)	0.1998(2)	0.2825(2)	0.33(5)
x=1.2						
Ca1	24*c*	1.0	1/8	0	1/4	0.49(4)
Sn1/Ti1	16*a*	0.8723/0.1277	0	0	0	0.356(11)
Al1/Ti2/Sn2	24*d*	0.6667/0.3148(16)/0.0185	3/8	0	1/4	0.43(6)
O1	96*h*	1.0	0.0975(2)	0.1999(2)	0.2827(2)	0.32(5)
x=1.4						
Ca1	24*c*	1.0	1/8	0	1/4	0.94(5)
Sn1/Ti1	16*a*	0.8000/0.2000	0	0	0	0.396(11)
Al1/Ti2/Sn	24*d*	0.6667/0.3333(15)/0.0000	3/8	0	1/4	0.14(6)
O1	96*h*	1.0	0.0978(2)	0.1999(2)	0.2828(2)	0.50(5)

Table 7
Bond lengths for $Ca_3Sn_{3-x}Ti_xAl_2O_{12}$.

Ti content, x	0.6	0.8	1.0	1.2	1.4
Ca–O (Å)	2.411(3) × 4	2.402(3) × 4	2.397(3) × 4	2.399(3) × 4	2.400(2) × 4
	2.554(3) × 4	2.549(3) × 4	2.556(3) × 4	2.553(3) × 4	2.551(3) × 4
〈Ca–O〉 (Å)	2.483	2.476	2.477	2.476	2.475
Sn1/Ti1–O (Å)	2.045(3) × 6	2.052(3) × 6	2.054(3) × 6	2.046(3) × 6	2.041(2) × 6
Al1/Ti2/Sn2–O (Å)	1.809(3) × 4	1.802(3) × 4	1.791(3) × 4	1.791(3) × 4	1.790(2) × 4

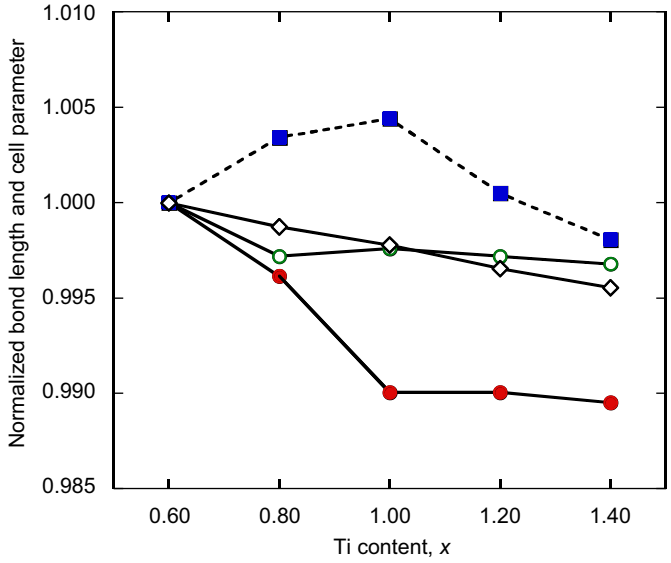

Fig. 6. Normalized cell parameter (◇) and *N* site-O1 distances of $Ca_3Sn_{3-x}Ti_xAl_2O_{12}$ as a function of Ti content *x*, *N*: Ca1 (○), Sn1/Ti1 (■), and Al1/Ti2/Sn2 (●).

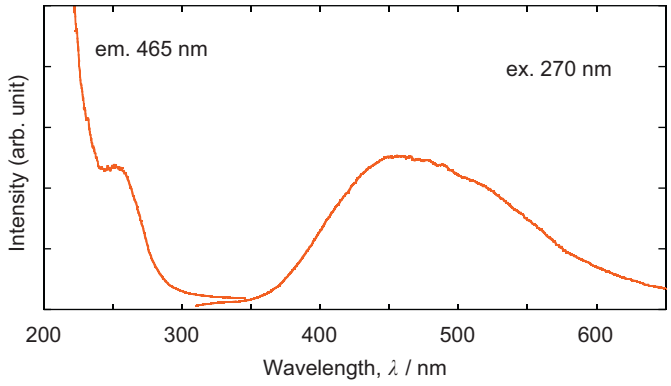

Fig. 7. PL excitation and emission spectra of $Ca_3Sn_{2.2}Ti_{0.8}Al_2O_{12}$ single crystals.

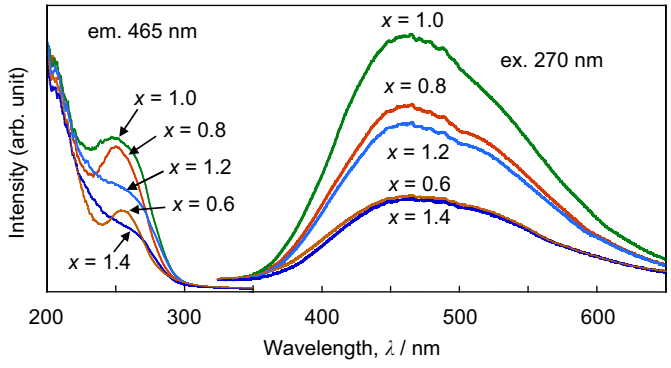

Fig. 8. PL excitation and emission spectra of polycrystalline $Ca_3Sn_{3-x}Ti_xAl_2O_{12}$.

kite-type phase and $CaAl_2O_4$. Garnet-type phase single crystals could not be obtained by slow cooling of this melt.

Since the reflections from the perovskite-type phase were very small, the compositions of the garnet-type solid solutions were regarded as being close to $Ca_3Sn_{3-x}Ti_xAl_2O_{12}$ with $x=0.4$–1.4. The nominal compositions of *x* were used for the Rietveld analysis. The cell parameters and *R* indices of the $Ca_3Sn_{3-x}Ti_xAl_2O_{12}$ are listed in Table 5. All powder data of the garnet-type solid solutions of $x=0.6$–1.4 were well analyzed, resulting in low values of *R* indices. As shown in Fig. 4, the cell parameters of the garnet phases obtained in the range from 0.4 to 1.4 linearly decreased with *x*. The refined site occupancies of Sn1/Ti1 and Al1/Ti2/Sn2, the atomic coordinates of O1 and the isotropic displacement parameters are shown in Table 6. The occupancies of Ti and Sn atoms in the tetrahedral Al1/Ti2/Sn2 site and Ti in the octahedral Sn1/Ti1 site are plotted against *x* in Fig. 5. A rise of Ti occupancies and the corresponding fall of Sn occupancies at the octahedral sites were in the range from $x=0.6$ to 1.0 and the gradual increase of Ti and decrease of Sn were from $x=1.0$ to 1.4. Ti occupancies at the tetrahedral sites started to increase greatly from $x=1.0$.

The Ca–O1, Al1/Ti2/Sn2–O1, and Sn1/Ti1–O1 distances are listed in Table 7. Fig. 6 shows the cell parameters and the distances normalized with the values of the sample with $x=0.60$. The Ca1–O1 distances are almost independent of *x* and the BVS calculated with the distances is almost equal to 2.0. A decrease of about 1% of Al1/Ti2/Sn2–O1 was observed from $x=0.60$ to 1.0, which may be caused by the preferential replacement of the large Sn atom at the Al1/Ti2/Sn2 site with a small Ti atom. Above $x=1.0$, the Al1/Ti2/Sn2–O1 disances were almost constant because most of the Sn atoms at the tetrahedral site had been substituted by Ti atoms.

3.3. Luminescence properties

Fig. 7 shows the PL excitation and emission spectra of the single crystals of $Ca_3Sn_{2.2}Ti_{0.8}Al_2O_{12}$. The crystals showed a broad emission band peaking at 465 nm under 270 nm excitation. An absorption band in the wavelength range of 240–290 nm with a peak at 255 nm is attributed to the CT transitions between Ti^{4+} and O^{2-}.

The PL excitation and emission spectra of the polycrystalline solid solution samples of $Ca_3Sn_{3-x}Ti_xAl_2O_{12}$ ($x=0.6$–1.4) are shown in Fig. 8. The spectra measured for the sample with $x=0.8$ well agreed with the spectra of the single crystals shown in Fig. 7. The excitation peak shifted from 260 to 250 nm with increasing *x* from 0.6 to 1.0, and the peak could not be clearly seen at $x=1.2$ and 1.4. The broad shape of the blue–white emission with a peak position of about 465 nm did not depend on the Ti content. The maximum emission intensity was observed for the sample with $x=1.0$, and a quantum efficiency of 0.15 was measured under 250 nm excitation at room temperature. The decreasing of the emission intensity above $x=1.0$ might be caused by concentration quenching associated with the increase of Ti occupancy in the 24*d* site, since the occupancy rapidly changed at and above $x=1.0$ as mentioned above.

Since the peak position (465 nm) and shape of the emission of $Ca_3Sn_{3-x}Ti_xAl_2O_{12}$ were independent of Ti^{4+} content x, we could not conclude which site contains the Ti^{4+} responsible for the emission. Similar broad emission with peak wavelengths of 445, 489, and 450 nm were measured by UV irradiation (240–270 nm) at room temperature for $Ca_2Sn_{1-x}Ti_xO_4$ [1], $CaSn_{1-x}Ti_x(BO_3)_2$ [4], and $Li_4Ge_5O_{12}$:Ti^{4+} [23], respectively. $Ca_2Sn_{1-x}Ti_xO_4$ and $CaSn_{1-x}Ti_x(BO_3)_2$ contain Ti^{4+} at octahedral sites. Ti^{4+} ions of $Li_4Ge_5O_{12}$:Ti^{4+} are doped at tetrahedral sites.

4. Summary

New garnet-type solid solutions were found in the CaO–Al_2O_3–TiO_2–SnO_2 system. Single crystals of $Ca_3Sn_{2.2}Ti_{0.8}Al_2O_{12}$ were obtained by the self-flux method using a starting mixture with a Ca and Al-rich composition. Solid solutions with nominal compositions $Ca_3Sn_{3-x}Ti_xAl_2O_{12}$ (x=0.6–1.4) were prepared by solid state reaction at 1370 °C. The cubic lattice parameters linearly decreased with increasing x. Sn^{4+} and Ti^{4+} partially occupy both tetrahedral and octahedral sites in the garnet-type structure. The solid solutions emitted blue–white light with a peak wavelength at 465 nm under UV irradiation.

Acknowledgment

This work was supported in part by the Global COE Program "Materials Integration, Tohoku University" and by a Grant-in-Aid for Scientific Research (B) (No. 21350113, 2009) from the Ministry of Education, Culture, Sports and Technology (MEXT), Japan.

Appendix A. Supplementary material

Supplementary data associated with this article can be found in the online version at doi:10.1016/j.jssc.2011.02.016

References

[1] T. Yamashita, K. Ueda, J. Solid State Chem. 180 (2007) 1410–1413.
[2] W.L. Konijnedki jk, Inorg. Nucl. Chem. Lett. 17 (1981) 129–132.
[3] S. Abe, H. Yamane, H. Yoshida, Mater. Res. Bull. 45 (2010) 367–372.
[4] T. Kawano, H. Yamane, J. Alloys Compd. 490 (2010) 443–447.
[5] T. Kawano, H. Yamane, Chem. Mater. 22 (2010) 5937–5994.
[6] R. Marchand, Y. Piffard, M. Tournoux, Acta Cryst. B31 (1975) 514–551.
[7] B. Cartie, F. Archaimbault, J. Choisnet, A. Rulmont, P. Tarte, I. Abs-Wurmbach, J. Mater. Sci. Lett. 11 (1992) 1163–1166.
[8] S. Geller, R.M. Bozorth, M.A. Gilleo, C.E. Miller, J. Phys. Chem. Solids 12 (1959) 111–118.
[9] A. Rulmont, P. Tarte, B. Cartié, J. Choisnet, J. Solid State Chem. 104 (1993) 165–176.
[10] P. Tarte, R. Cahay, A. Garcia, Phys. Chem. Miner. 4 (1979) 55–63.
[11] H. Yamane, S. Abe, R. Tu, T. Goto, Acta Cryst. E66 (2010) i72.
[12] D.A. Jerebtsov, G.G. Mikhailov, Ceram. Int. 27 (2001) 25–28.
[13] PROCESS-AUTO, Rigaku/MSC, 9009 New Trails Drive, The Woodlands, TX 77381-5209, USA and Rigaku, 3-9-12 Akishima, Tokyo 196-8666, Japan. Rigaku/MSC & Rigaku Corporation, 2005.
[14] T. Higashi, NUMABS—Numerical Absorption Correction, Rigaku Corporation, Tokyo, 1999.
[15] G.M. Sheldrick, Acta Cryst. A64 (2008) 112–122.
[16] L.J. Farrugia, J. Appl. Cryst. 32 (1999) 837–838.
[17] K. Momma, F. Izumi, J. Appl. Cryst. 41 (2000) 653–658.
[18] F. Izumi, K. Momma, Solid State Phenom. 130 (2007) 15–20.
[19] N.E. Brese, M. O'Keeffe, Acta Cryst. B47 (1991) 192–197.
[20] S. Geller, Z. Krist. 125 (1967) 1–47.
[21] R.P. Gunawardane, J.G. Fletcher, M.A.L. Dissanayake, R.A. Howie, A.R. West, J. Solid State Chem. 112 (1994) 70–72.
[22] J.A. Bland, Acta Cryst. 14 (1961) 875–881.
[23] W.C. Wong, T. Danger, G. Huber, K. Petermann, J. Lumin. 72–74 (1997) 208–210.
[24] R.A. Young, in: R.A. Young (Ed.), The Rietveld Method, Oxford University Press, Oxford, 1993, pp. 1–38.